



Acrylic polymer/TiO₂ nanocomposite coatings: Mechanism for photo-degradation and solar heat reflective recovery

Phi Hung Dao^a, Thien Vuong Nguyen^{a,b,*}, Tuan Anh Nguyen^a, Thi Yen Oanh Doan^c, Thu Ha Hoang^d, The Tam Le^e, Phuong Nguyen-Tri^f

^a Institute for Tropical Technology, VAST, 18 Hoang Quoc Viet, Cau Giay, Hanoi, 10000, Viet Nam

^b Graduate University of Science and Technology, VAST, 18 Hoang Quoc Viet, Cau Giay, Hanoi, 10000, Viet Nam

^c Publishing House for Science and Technology, VAST, 18 Hoang Quoc Viet, Cau Giay, Hanoi, 10000, Viet Nam

^d University of Education - Vietnam National University, 144 Xuan Thuy, Cau Giay, Hanoi, 10000, Viet Nam

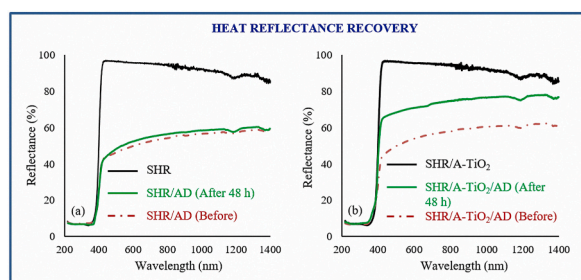
^e Vinh University, 182 Le Duan, Vinh city, Nghean, Viet Nam

^f Department of Chemistry, Biochemistry and Physics, Laboratory of Advanced Materials for Energy and Environment, Université du Québec à Trois-Rivieres, Québec, Canada

HIGHLIGHTS

- Nano-A-TiO₂ inhibited the transformation of chemical structure and weight loss of acrylic coating.
- New degradation mechanism of acrylic polymer/A-TiO₂ nanocoating was proposed.
- Nanocoating significantly recovered the heat reflectance of solar heat reflective system.

GRAPHICAL ABSTRACT



ARTICLE INFO

Keywords:
 Photocatalytic degradation
 Water-based acrylic coating
 Self-cleaning ability
 Heat reflectance recovery

ABSTRACT

This work focuses on the degradation mechanism and self-cleaning ability of acrylic/A-TiO₂ nanocomposite coating.

In the study of photocatalytic degradation, Infrared spectroscopy (I.R.) data indicated that both the losses of alkane C.H. group, the weight and transparency of nanocomposite coating increased with increasing the nanoparticle content. To explain this finding, we proposed a new degradation mechanism for this water-based acrylic/A-TiO₂ nanocomposite coating.

The experimental data confirmed a high self-cleaning ability of the as-prepared coating to remove both methyl blue and artificially dirt mixtures for the self-cleaning test. As observed, methyl blue content has been degraded after 12 h of U.V. exposure. Furthermore, when used this nanocomposite coating as a topcoat in the Solar heat reflectance (SHR) coating system, after 48 h of U.V. exposure, the heat reflectance of the SHR coating system was highly recovered from 59% to 76%, due to the self-cleaning activity of nano-topcoat. Whereas, without topcoats, the heat reflectance of SHR coating was weakly retrieved from 57% to 61%.

* Corresponding author. Institute for Tropical Technology, VAST, 18 Hoang Quoc Viet, Cau Giay, Hanoi, 10000, Viet Nam.
 E-mail address: vuongvast@gmail.com (T.V. Nguyen).

1. Introduction

Tropical climate refers to the weather condition with various typical parameters, such as (i) a high number of sunny hours, (ii) high temperature and (iii) high humidity, which facilitate the development of microorganisms/fungi on the surface of materials and productions. Traditional surface cleaning methods have been used under high risk of working accidents with high cost, for example, on the glass walls outdoor of high-rise buildings. Hence, applying the self-cleaning coating on the surface of materials/productions is necessary, not only for the safety/security reason but also for the economic/social impact.

Nanotechnology has played a crucial role in the development of sciences and societies recently. With the rapid growth of coating technology, inorganic nanoparticles have been added into coating formulations to produce multi-functional coatings, such as shielding U.V. coating [1], self-cleaning coatings, and antibacterial coatings [2–6]. They are also reported to enhance the mechanical and thermal properties of coatings [7–9] and improve their weather durability [10,11]. In general, there are two main approaches to fabricate the self-cleaning coatings via nanotechnology: i) approach by lotus leaf effect provided by nanostructure/hierarchical structure, and ii) approach by the photocatalytic mechanism of nano-photocatalysts. A super-hydrophobic organic coating can be produced on the outdoor surface in the lotus leaf effect, significantly reducing the effective cost of maintaining and cleaning processes [12,13]. In this direction, SiO₂ nanoparticles have been used widely with various polymers (thermos-plastic elastomers, fluorinated polysiloxane, polyurethane) to provide the super-hydrophobic property. In the literature, recent studies reported the use of castor oil and hydrophobic SiO₂ nanoparticles to fabricate the super-hydrophobic eco-friendly organic coatings [14,15].

In the case of photocatalytic mechanisms for self-cleaning purposes, ZnO [16,17] and A-TiO₂ [18–21] nanoparticles have been considered promising nano-photocatalysts. In this regard, pollutants and contamination can be degraded by nanoparticle-induced photocatalysis under U. V. light irradiation. Moreover, the surface of the nanocomposite coating becomes more hydrophilic by producing more hydroxyl and carboxyl under the photocatalytic effect under U.V. light radiation. Hence, rain-water creates a stream on the surface of nanocomposite coating, eroding contamination. Experimental data indicated that A-TiO₂ has higher photocatalytic activity than nano-ZnO. As a result, A-TiO₂ nanoparticles (nano-A-TiO₂) have been used intensively for practical applications [22], especially environmental remediation [23], wastewater treatment, soil/air remediation [24,25]. It was also reported in the literature that nano-A-TiO₂ provided the self-cleaning layer for surfaces of photovoltaic devices. The authors successfully fabricated the nanocoating with suitable optical property and high transmittance (>99% of the transmittance) [26]. Acayanka et al. also used nano-A-TiO₂ to produce self-cleaning clothes with the presence of visible light. The authors reported that nano-TiO₂ coated textiles could degrade pollutants. In the study of Zanfir et al. [27], Remazol Brilliant-R (RBB-R) and RBB-R dyes were completely removed after 5 h of sunlight irradiation with the presence of acetone/water (50:50) mixture [27]. Besides, TiO₂/silica fume hybrid could be used to fabricate the self-cleaning mortar. As reported, with 3 wt% of these nanoparticles, compressive strength has been significantly increased, but their hardening time became more prolonged than the neat mortar [27].

Overall, the high photocatalytic activity of nano-A-TiO₂ has two sides when used in organic nanocoating. On the negative side, it could promote the photo-degradation of polymeric matrices. Therefore, the mechanism for degradation of polymer/A-TiO₂ nanocomposite coating has been proposed in the literature. Briefly, the mechanism of photo-degradation of this polymer/TiO₂ nanocoating can be described by the following stages: electrons (e⁻) of TiO₂ absorbs energy from light irradiation and jump to a higher level of energy (in the conduction band), thus leaving a hole (in the valence band) (h⁺) containing the positive charge. After that, particles containing charge would combine with

oxygen, water to produce free radical and protons. This mechanism could be applied to both nano-ZnO, nano rutile-TiO₂. However, in our previous studies on the ageing process of nano-ZnO/rutile-TiO₂ acrylic nanocomposite coatings, we demonstrated that nano-ZnO produces much more hydroxyl groups and conjugated carbon double bonds than R-TiO₂ nanoparticles upon accelerated weathering test [1]. Moreover, Chen et al. [28] signalled that nano-A-TiO₂ provided a much better photocatalytic property than rutile TiO₂ [28]. Therefore, the degradation mechanism of polymeric nanocoatings depends on both types of nanoparticles/nano-phocatalysts and polymer matrix. In this work, the water born nanocomposite coatings have been prepared using AC 261 acrylic emulsion and A-TiO₂ nanoparticles. Their aging process was then investigated by I.R. analysis, weight loss, scanning electron microscopy (SEM). In addition, the self-cleaning activity of these acrylic nanocoatings was evaluated when used as the topcoat for solar heat reflectance (SHR) paint system in the presence of artificial dirt.

2. Experimental

2.1. Materials

PRIMAL™ AC-261 acrylic emulsion with 50 wt% solid content and coalescing agent of texanol (2,2,4-trimethyl-1,3-pentanediol monoisobutyrate) were supplied by Dow Chemical – USA. Nano-A-TiO₂ (diameter < 100 nm; specific surface area of 18 m²/g) was purchased from Sigma Aldrich (Singapore). Methylene blue (M.B.) was obtained from Merck -Germany, and some other chemicals such as ethanol, carbon black and silica dye were used in this study. TiO₂ powders were obtained from Dupont R92, and Hollow microspheres were supplied by Hy-Tech (USA).

2.2. Samples preparation

In this work, 2,2,4-trimethyl-1,3-pentanediol monoisobutyrate (texanol) was used at a content of 3 wt% to improve the coalescing ability of the paint [1,10,29]. Nano-A-TiO₂ was incorporated into the coating formulations at 0.5, 1, 2 and 4 wt%. Distilled water was added at 20 wt% (by weight of the total solid resin).

The coating formulations were fabricated following various steps. At first, ultrasonic-assisted (35 Khz) dispersion of nano-A-TiO₂ into distilled water (called batch A) and hexanol into the acrylic emulsion (called batch B) have been carried out (1 h under ultra-sonication). After that, the mixture of batch A and batch B was carried out under ultra-sonication for 3 h.

For UV-Vis, I.R. analysis, weight loss measurements and photocatalytic tests, various coatings were deposited on the glass plates (100 × 70 × 2 mm) on a quadruple film applicator (Erichsen model 360, Germany). After drying in the air (7 days), the dried films were taken out of the glass plates for further tests (average thickness of ~25 μm).

Methylene blue (M.B.) was used for self-cleaning tests. First, M.B. was used in solution with ethanol at 1 mM of concentration, prepared by dissolving in ethanol stirred by Ika RW16 Basic Mixer (England) for 2 h. Then, this M.B. solution is sprayed on the coating with and without A-TiO₂ which were fabricated on the glass substrate using the quadruple film applicator (Erichsen model 360, Germany), followed by vacuum drying at 60 °C.

Solar-heat reflective paint was prepared from a mixture of AC-261, Rutile TiO₂ powder, Hy-Tech hollow microspheres and nano-SiO₂ with a 100/80/20/2 wt ratio. The solar-heat reflective coating was prepared as described in a method published in a recent article [5].

The self-cleaning performance of nanocomposite coating in the solar-heat reflective coating system has been carried out by monitoring UV-vis-NIR reflectance with the presence of an artificial dirty mixture on its surface. Solar-heat reflectance coating systems (on glass substrate) consisted of two layers: i) solar-heat reflective coating with 120 μm thickness as a base coat and ii) A-TiO₂-nanocomposite coating with 25

μm thickness as the topcoat. The artificial dirt solution (at the concentration of $2 \text{ mL}/\text{cm}^2$) was applied on the surface of the as-prepared coating system. As modified from Ref. [30], the artificial dirty solution was prepared by mixing 85 wt% nano-clay, 12 wt% nano-silica s, 1 wt% carbon black and 2 wt% oil, and 15 g/L distilled water. After drying at room temperature, the investigated samples were exposed to U.V. light. It is noted that this test procedure did not include a condensation process to avoid the further erosion of artificial dirt that would cause a negative effect on results. Reflectance spectra were evaluated by using UV-Vis-NIR spectroscopy meter (UV2600, Shimadzu, Japan).

2.3. Analysis and test

2.3.1. Accelerated weathering study

The ageing of the coatings was evaluated in an Atlas UVCON weathering chamber (model UC-327-2) equipping UVA-340 fluorescent lamps with the operating condition below: (i) wet-cycle conditions for 8 h under U.V. exposure with the temperature of 60°C at the black panel; (ii) following by the water condensation in the dark (CON) for 4 h with the temperature of 50°C . Thus, one cycle of accelerated weathering consists of 8 h U.V. and 4 h CON. The self-cleaning examinations were carried out at 60°C for 48 h only under U.V. radiation without condensation to avoid the removal of artificial dirt by water. All samples before and after testing were dried and stabilized in a vacuum oven at 60°C for 24 h before the analysis.

The self-cleaning property of A-TiO₂ nanocoating was evaluated under U.V. irradiation exposure at 60°C for 48 h. In this case, we did not use the condensation stages to avoid the possibility of artificial dirt washed away by the condensation water.

2.3.2. Characterizations

a) I.R. analysis

I.R. measurement has been used to evaluate the chemical changes of coatings during the UV/CON test. FTIR spectroscopy has been collected using the NEXUS 670 Nicolet, equipped by detector DTGS-KBr at the resolution of 4 cm^{-1} and 16 scans at transmission mode (without using KBr).

To analyze the variation of the characteristic peaks of the coating samples, we recorded I.R. spectra at the various ageing times through the discrete intervals of measurements on the same spot for each coating. From the variation in structural bands of I.R. spectra, the relative contents of the remaining functional groups were calculated by the ratio below [10]:

$$\text{Remaining group (\%)} = (D_t/D_0) \times 100\%$$

Where:

D_t : Absorbance of the exposed coating after time t

D_0 : Absorbance of the unexposed coating

b) Weight loss of coating samples

Before the measurements, all coating samples were dried using a vacuum oven at 60°C until reaching their constant weight. The weight loss (Δm_t) of these coatings after weathering test was estimated by the following equation [10]:

$$\Delta m_t (\%) = [(m_0 - m_t)/m_0] \times 100$$

Where:

m_0 : Weights of coating sample before the exposure

m_t : Weights of the samples after the g exposure

The instrument (balance) employed for the weight loss

measurements of coating samples was Ohaus® Pioneer® Plus analytical balance (Ohaus Corporation, New Jersey, United States), Model PA214, weighing capacity 210 g, resolution: 0.1 mg).

c) Morphological analysis

The surface morphology of coating samples was examined by using a Field Emission Scanning Electron Microscopy (FE-SEM, Hitachi S-4800, Japan).

2.3.3. Self-cleaning performance

The self-cleaning activity of the nanocomposite coating was tested with the presence of M.B. and an artificial dirty mixture.

a) With the presence of methyl blue

The discolourations of M.B. during the photocatalytic examination were performed according to ASTM D2244.

The reduction of absorbance for the chromospheres in M.B. was evaluated by using the U.V.-Vis spectrophotometer (GBC, CINTRA 40, USA) with 2 nm slip width and the transmission geometry.

b) With the presence of an artificial dirty mixture

The self-cleaning activity of the nanocomposite coatings for the artificial dirty mixture was assessed by a method based on its heat reflectance recovery for solar-heat reflectance coating system using UV-Vis-NIR spectroscopy meter (UV 2600, Shimadzu, Japan).

3. Results and discussions

3.1. Photocatalysis degradation of water-borne acrylic polymer/A-TiO₂ nanocomposite coating

3.1.1. Effect of nano-A-TiO₂ on the chemical change of coatings

The changes of functional groups can be used to evaluate the degradation degree of the coating upon accelerated weathering test. The I.R. spectra of water-borne acrylic coatings unfilled and filled 0.5, 1, 2 and 4 wt% A-TiO₂ nanoparticles before and after 24 cycles of UVA/CON accelerated weathering tests were represented in Fig. 1.

As shown in Fig. 1, certain intensity changes of some peaks were observed for the coatings due to ageing testing. The interesting finding is that the I.R. transparency of the coatings and the intensity of the band at 2945 cm^{-1} assigning to alkanes C.H. group decreased seriously with increasing the content of nano A-TiO₂.

One possible explanation for these obtained results is that nano A-TiO₂ could act as a photocatalyst in the ageing process of nanocomposite coatings. Thus, the surface of the nanocomposite coating becomes much rougher and more porous, resulting in an increase of light scattering, then the amount of light passing through the nanocomposite coating decreases.

To analyze the chemical changes of coating samples quantitatively during the photo-degradation test, we focus on the I.R. characteristic bands of alkane C.H. located at 2945 cm^{-1} (Fig. 2).

As can be seen in Fig. 2, the mentioned hypothesis may be appropriated. Because, in the presence of nano A-TiO₂ the functional groups of nanocomposite coating changed significantly, i.e. the remaining alkane (C-H) of the neat aged coating was 78%, while the remaining C-H of aged nanocomposite coatings containing 0.5, 1, 2 and 4 wt% nano A-TiO₂ were 74, 71, 67 and 65%, respectively.

In our previous studies, R-TiO₂ nanocomposite coating presented a lower degradation degree than neat coating upon ageing process [1,10]. Thus, it can be explained that while R-TiO₂ nanoparticles illustrate UV-absorber activities, A-TiO₂ played a role as photocatalyst in the ageing process of nanocomposite coating, which promoted the degradation of nanocomposite coating. This finding is compatible with the

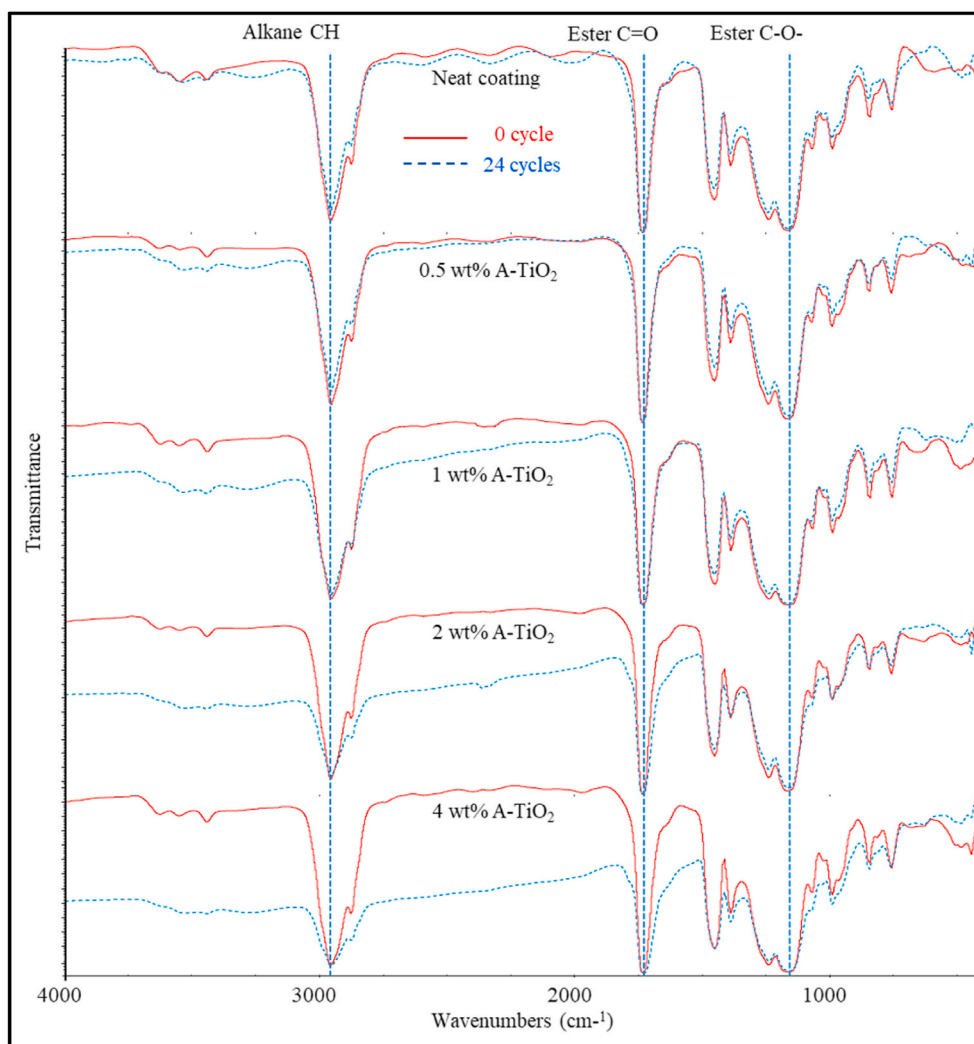


Fig. 1. Infrared spectra of neat coating and coatings containing A-TiO₂ nanoparticles at various contents before and after 24 cycles of accelerated weathering test.

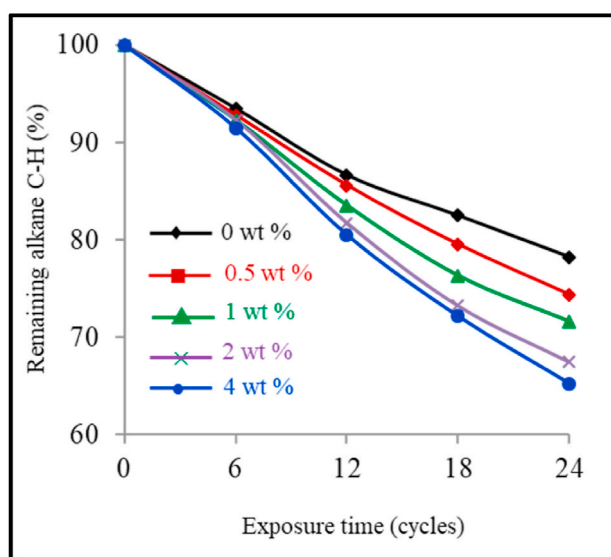


Fig. 2. Chemical change after accelerated weathering test for the neat and nanocomposite coatings.

reported results by Chen et al. [28].

3.1.2. Effect of nano-A-TiO₂ on the weight loss of the coating

Coatings exposed by U.V. irradiation, high humidity and temperature, were degraded due to photo-degradation and hydrolysis in the condensation stage leading to chemical changes, firstly leading to low molecular weight, and then the coating eroded. Consequently, the thickness and the weight of the coating decreased. Therefore, monitoring the weight of coating during weathering tests as one of the useful methods is used to examine the degradation of coating [31,32]. The weight loss of formula coatings during the accelerated weathering test was presented in Fig. 3.

As can be seen in Fig. 3., the weight of samples is reduced with different degrees. Weight loss is raised with the increase of A-TiO₂ content. After 24 cycles of weathering tests, neat coating lost nearly 10% of its weight while nanocomposite coating loaded 4 wt% A-TiO₂ showed the highest weight loss among investigated coatings, i.e., 30%. The weight loss of investigated coatings can be arranged as A-TiO₂ content: 0 wt % (Neat coating) < 0.5 wt% < 1 wt% < 2 wt% < 4 wt%. It is observed that there was a little difference between the weight loss of nanocomposite coating loaded 2 wt% and 4 wt% A-TiO₂. It can be explained that in high content, A-TiO₂ nanoparticles can be easily agglomerated to produce larger grain and thus reducing nanoparticles performance [1,10].

The investigated coatings indicated higher degradation with

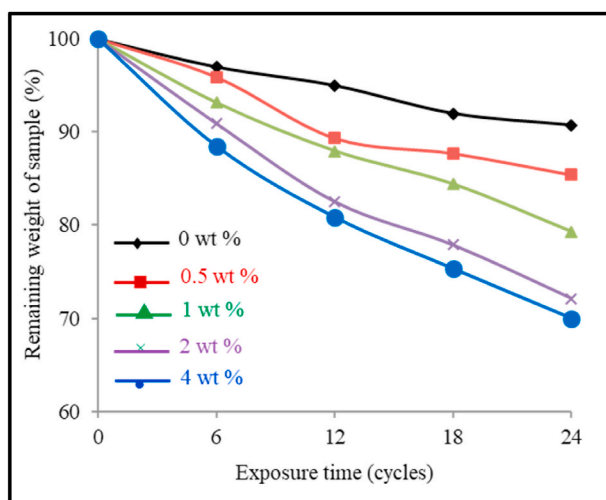


Fig. 3. Influence of nano-A-TiO₂ on weight loss of the coating samples during UV-A/CON aging test.

increasing A-TiO₂ content. In other words, A-TiO₂ enhanced the coating degradation due to photocatalytic activity. FE-SEM images of neat coatings and nanocomposite coating loaded 2 wt% were displayed in Fig. 4.

It is evident that the surfaces of investigated coatings were reasonably smooth. However, the surface became much rougher than that initial one, especially in terms of nanocomposite coating. The surface of aged nanocomposite coating loaded 2 wt% A-TiO₂ nanoparticles were damaged at a much high level compared to the surface of the neat aged coating. It can be easily explained that A-TiO₂ plays the role of a

photocatalytic agent and thus encouraging the degradation of nanocomposite coatings during accelerated weather tests. The morphology can investigate the hypothesis mentioned above that the baseline of I.R. spectra of aged nanocomposite coating reduced compared to initial ones. The surface of nanocomposite coatings was damaged and became much rougher and thus increasing the amount of reflectance and scattering light. In other words, the surface of aged nanocomposite coating reduced the amount of I.R. light transmittance.

Fig. 5 presents UV-vis spectra (in the transmission mode) of neat coating and coating containing 2 wt% A-TiO₂ nanoparticles before and after 24 cycles of accelerated weathering test.

As shown in Fig. 5, the transparency of nanocomposite coating decreases clearly after 24 ageing cycles, whereas it is slightly reduced for the neat coating.

Similarly, in the FE-SEM images (Fig. 4), the nanocoating degradation behaviour mainly occurred on the surface areas, where the nanoparticles were directly exposed to UVA ultraviolet light. As a result, these surface areas were worn away, but no cracks could be observed.

By combining the obtained data from I.R. analysis, weight loss measurement and morphological study, we propose the mechanism for coating degradation induced by A-TiO₂ nanoparticles (Fig. 6).

As shown in Fig. 6, TiO₂ nanoparticles absorb energy from photons of U.V. light to produce electrons at excited status and jump to the conduction band, consequently leaving holes containing a positive charge. After that, particles containing charge combines with water and oxygen to produce free radical and protons. Active free radical like O.H.^{*} attacked the polymer chain of acrylic emulsion producing R₁OH and free radical P^{*}. However, free radical P^{*} is not stable. P^{*} immediately combines with oxygen, producing free radical POO^{*}. That is why the weight of coatings increased in the first period of the ageing process, as Chen et al. [28] discovered in the case of polyurethane coating. However, the phenomenon of weight loss was not observed for the coatings

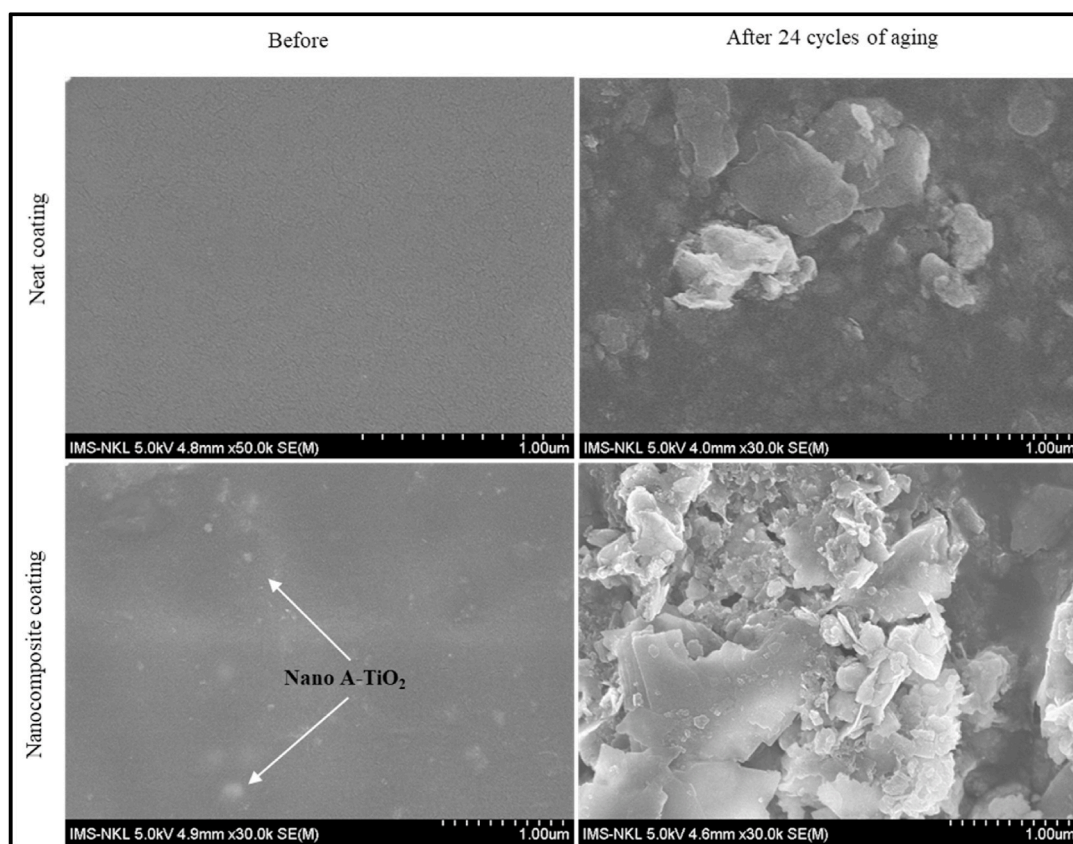


Fig. 4. FE-SEM images of the neat coating and its nanocomposite containing 2 wt % A-TiO₂ nanoparticles before and after 24 cycles of accelerated weathering exposure.

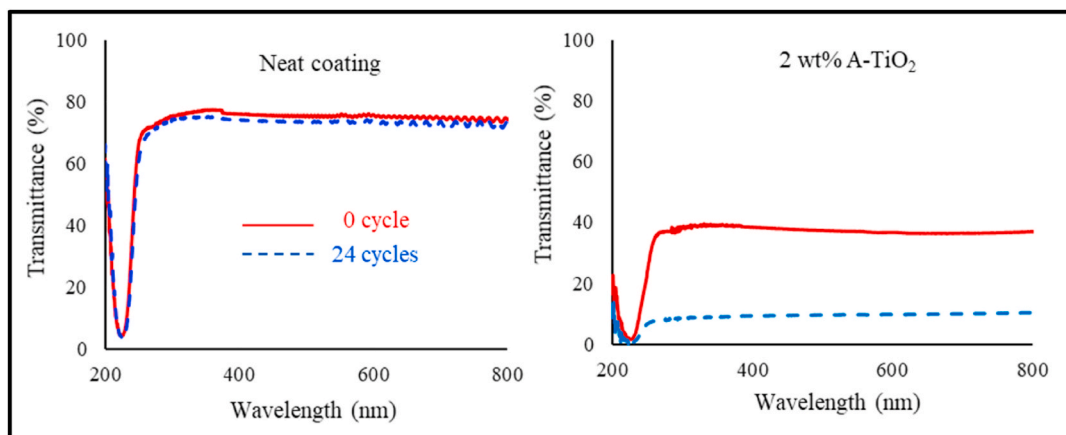


Fig. 5. UV-vis spectra (in the transmission mode) of neat coating and coating containing 2 wt% A-TiO₂ nanoparticles before and after 24 cycles of accelerated weathering test.

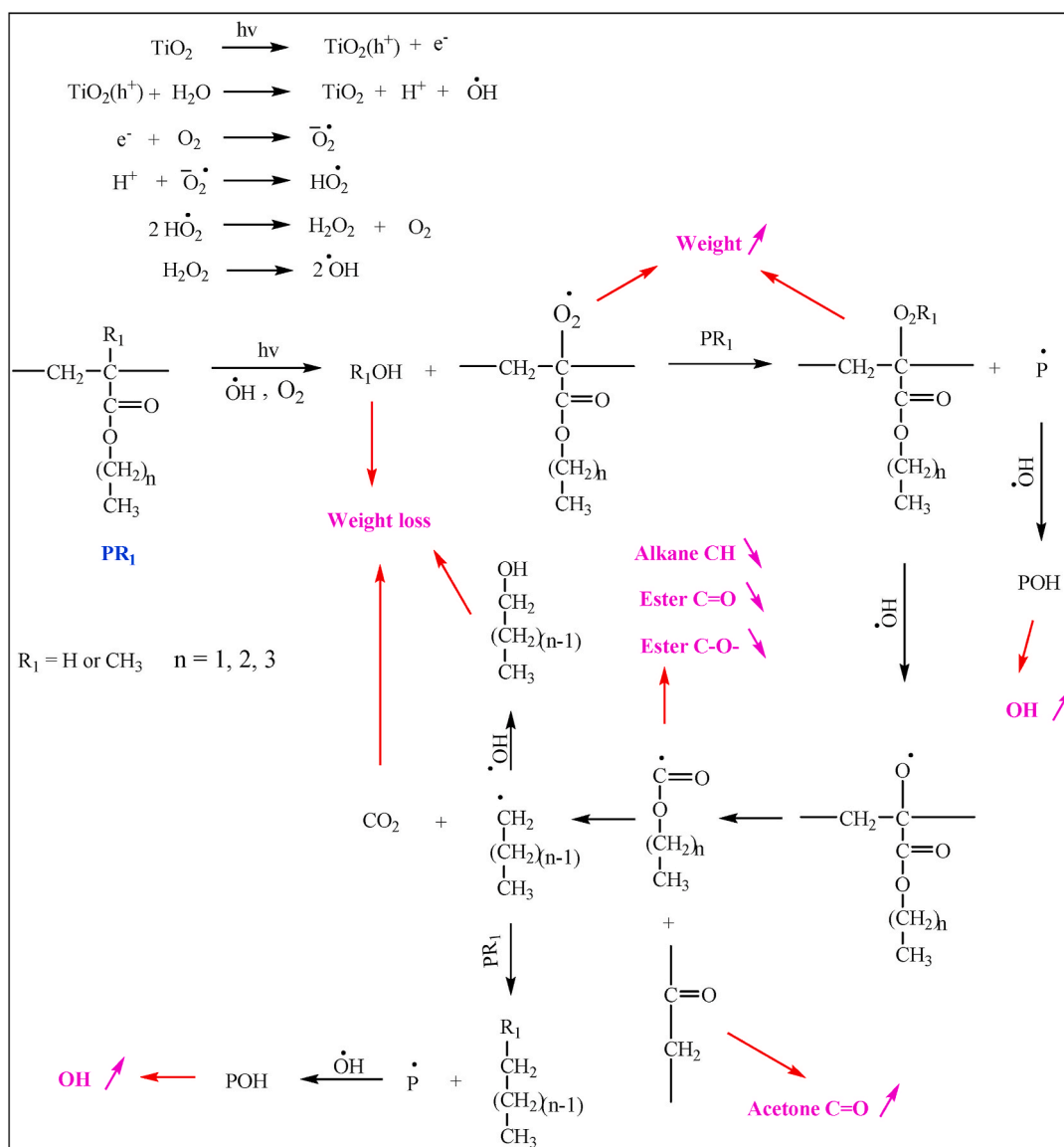


Fig. 6. Mechanism for photocatalytic degradation of water-borne acrylic polymer/A-TiO₂ nanocomposite coating.

in this work, possibly because POO* reacted fast with polymer chains to produce water or alcohol R_1OH . As a result, the weight of the coatings reduced quickly upon the aging process and reduced functional groups such C.H., ester C=O and ester C-O. As the mechanism proposed hydroxyl mainly produced in the form of water and alcohol easily washed by water in the condensation cycle, the intensity of the hydroxyl in aged formula coatings insignificantly increased.

In terms of neat coating, the mechanism of coating degradation occurs through two steps [33]: (i) e_{π} of ester groups receive energy from U.V. light and jump to high levels of energy (π^*), consequently, the polymer chain scission occurs to produce free radical R_1^* and P^* . Then P^* immediately reacts with oxygen to produce peroxide, which is the reason coating weight increases. And R_1^* can react with water to produce R_1H and free radical $O.H.^*$ and peroxide (ii) free radical attacks to polymer chain leading to scissions of the polymer chain by photolysis and hydrolysis reactions. As a result, low molecular weight oxidation products are possibly produced. These low molecular products can either evaporate or be washed away by moisture in the air, thus losing the coating material.

As the mechanism of coating degradation, in the presence of A-TiO₂ nanoparticles, nanocomposite coating degradation is enhanced. The degradation degree of nanocomposite coating increases with growing A-TiO₂ content. It means A-TiO₂ nanoparticles play as photocatalysts and thus producing much more free radicals. Consequently, the degradation of nanocomposite coating was much higher than degradation of the neat coating.

3.2. Self-cleaning performance of the nanocomposite coating

3.2.1. Photocatalysis performance of nanocomposite coating for methylene blue decomposition

The photocatalysis performance of the coatings was investigated by decomposition of methylene blue (M.B.) dye. M.B. was dissolved in ethanol at 1 mM and was sprayed on samples coated by a neat coating and nanocomposite containing 2% nano A-TiO₂. The studied samples were exposed to U.V. light which was 340 nm of wavelengths. The change of M.B. was monitored by the colour and U.V. spectroscopy measurement. b^* value in colour measurement and U.V. spectrum of samples coated M.B. following U.V. exposure time was displayed on Figs. 7 and 8, respectively.

As shown in Fig. 7, the minus of b refers blue and plus of b value refers to yellow. Thus, the blue of M.B. of both samples reduced in late 4 h U.V. irradiation. Then, the b^* value of sample unfilled A-TiO₂ changed

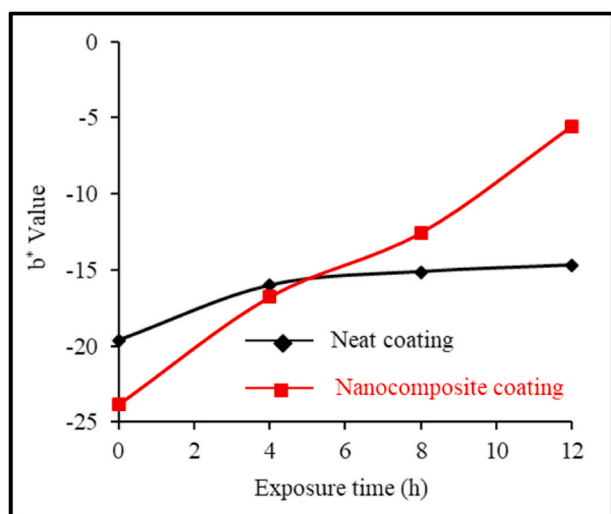


Fig. 7. b^* value of with and without A-TiO₂ coated M.B. during U.V. exposure test.

slightly while the b^* value of sample filled A-TiO₂ still dramatically increased. Hence, it can explain that M.B. was degraded significantly in the presence of A-TiO₂. Therefore, this hypothesis seems to be appropriate.

The MB degradation upon U.V. irradiation was also measured by UV-Vis spectroscopy. U.V. spectrum of sample coated M.B. in the absence of A-TiO₂ showed that M.B. had an absorbance at 560 nm. This peak was sharp while the absorbance of samples with A-TiO₂ became wider and reached a peak at nearly 600 nm. Therefore, it may be an effect of A-TiO₂. As can be seen from Fig. 6, the content of M.B. reduced significantly after 4 h exposure for both samples. And then, the content of M.B. was fairly stable for samples without A-TiO₂ while the content of M.B. still decreased more deeply. After 12 h of U.V. irradiation, the peak of MB at 600 nm was insignificant for sample filled A-TiO₂. This result is following the hypotheses mentioned above.

3.2.2. Self-cleaning performance of the nanocomposite coating for artificial dirt

Nowadays, environmental issue such air pollution, climate change has been alarmed over the world. Governments worldwide have been attempting to improve the environment via different approaches i.e. reducing greenhouse gas and using some functional coating to decrease pollutants in the air. However, global warming and energy security nowadays have become challenging. Hence, the solar-heat reflective paint system becomes an interesting topic for both scientists and industrialists. Solar-heat reflective paint can save up to 190 kWh/m²/year [34], providing energy security. However, the solar-heat reflective coating is strongly affected by contamination on its surface. This work presents the test which examined the self-cleaning ability of A-TiO₂ nanocomposite coating. The test includes two coating systems consisting of solar-heat reflective coating (SHR) and solar-heat reflective coating based on coat and A-TiO₂ nanocomposite coating as topcoat (SHR/A-TiO₂). Both coating systems were coated with artificial dirt (2 mL/cm²). Reflectance spectra were measured before and after 48-h U.V. exposure using a UV-Vis-NIR spectroscopy meter (UV2600, Shimadzu, Japan). The UV-Vis-NIR spectra of SHR, SHR/A-TiO₂ system initial, coated by artificial dirt before and after 48-h U.V. exposure was presented in Fig. 9.

As shown in Fig. 10, the reflectance of SHR in the range of 700–1400 nm was fairly high, reaching 90.5. After applying composite coating loaded 2% A-TiO₂, the reflectance of the system changed insignificantly (from 90.5 to 91%). When the artificial dirt was applied, the reflectance of both systems decreased significantly, i.e. 57 for SHR and 61 for SHR/A-TiO₂ (the difference between SHR coated dirt and SHR/A-TiO₂ coated dirt was the cause of the standard error). After U.V. treatment, the reflectance of both systems recovered with different degrees. SHR showed a slight increase to 59, which is explained due to the bonds of inorganic contamination to coating surfaces broken by the U.V. light irradiation, while the reflectance of SHR/A-TiO₂ recovered to 76% after 48-h U.V. exposure. The photocatalytic properties of nano TiO₂ can photo-oxidize organic and inorganic contamination [35], and A-TiO₂ nanocomposite plays the role of self-cleaning coating. That also proves that A-TiO₂ nanocomposite can be applied as a topcoat for the SHR system because it doesn't affect the reflectance of SHR coating initially but also contributes to recovering reflectance of SHR coating strongly. Based on this exciting finding, the practical use of this A-TiO₂ nanocomposite coating as a topcoat for SHR system is auspicious.

4. Conclusion

The photocatalytic degradation and self-cleaning performance of water-borne acrylic polymer/A-TiO₂ nanocoatings were investigated via various characterization techniques. The obtained results on their changes in chemical structure, weight and morphology during the ageing process indicate that A-TiO₂ nanoparticles significantly enhance the photocatalytic degradation of acrylic coatings. FE-SEM observation indicates that nanocoating degradation mainly carries out on the surface

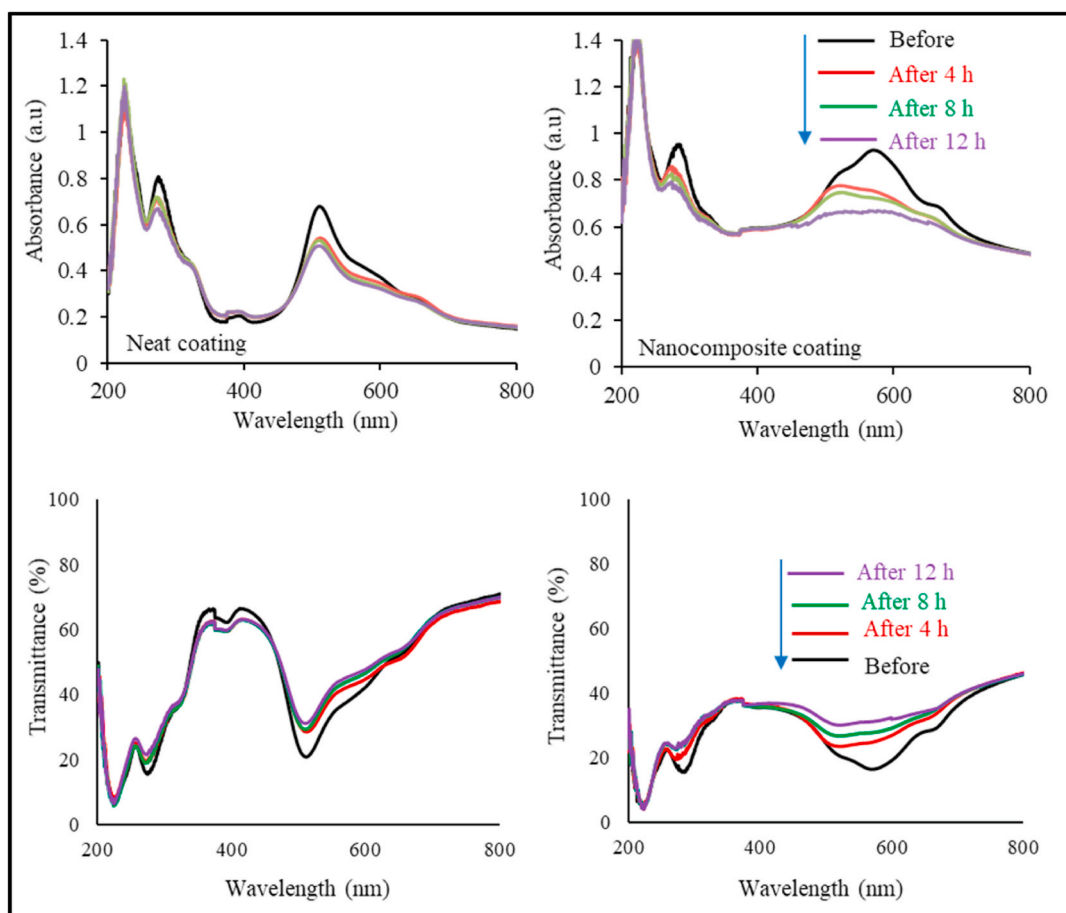


Fig. 8. UV-vis spectra of coatings with and without A-TiO₂ coated M.B. during U.V. exposure test.

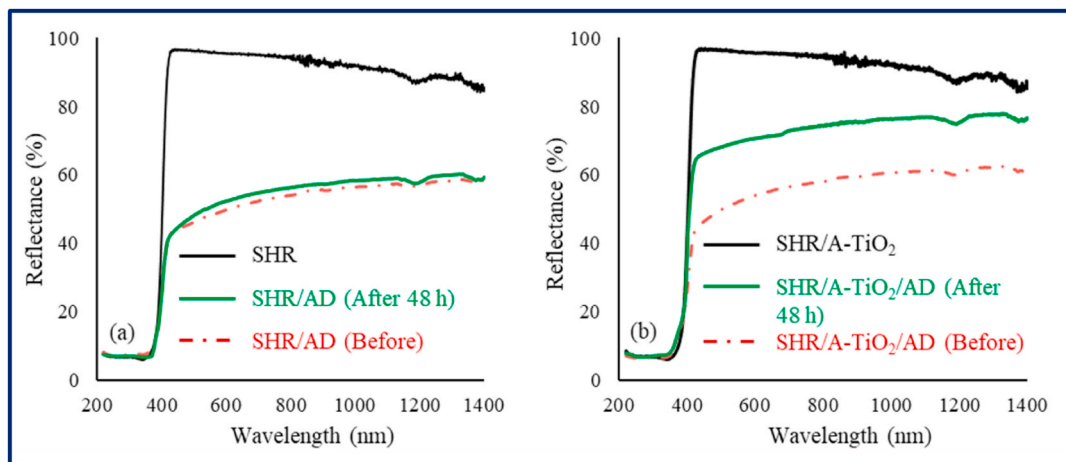


Fig. 9. UV-Vis-NIR spectrum of solar-heat reflective coating systems-before and after 48 h U.V. light irradiation: a) without nanocoating as top-coated; and b) with nanocoating as top-coated. Where, SHR: solar-heat reflectance coating; nano-A-TiO₂ (topcoat): acrylic polymer/A-TiO₂ nanocomposite coating; A.D.: artificial dirt.

areas, where the nanoparticles expose directly to the U.V. light. These degraded surface areas are worn away, similar to the sacrificial layer under self-cleaning activity. Besides, no cracking could be observed on the surface of nanocoating. A newly proposed degradation mechanism of this nanocoating was discussed in detail. The nanocoating had a high self-cleaning performance for methyl blue and artificial dirt mixture. Due to the self-cleaning activity of nanocoating as a topcoat, the heat reflectance of the SHR heat reflective coating was strongly recovered from 59% to 76% only after 48 h of U.V. exposure. Without the topcoat,

the heat reflectance of the SHR coating can only be slightly restored from 57% to 61%. As the smart coating, this acrylic polymer/A-TiO₂ nanocoating exhibits high reflectivity recovery for solar heat-reflective coating.

CRediT authorship contribution statement

Phi Hung Dao: Formal analysis, Data curation, Writing – original draft, Approval of the version of the manuscript to be published. **Thien**

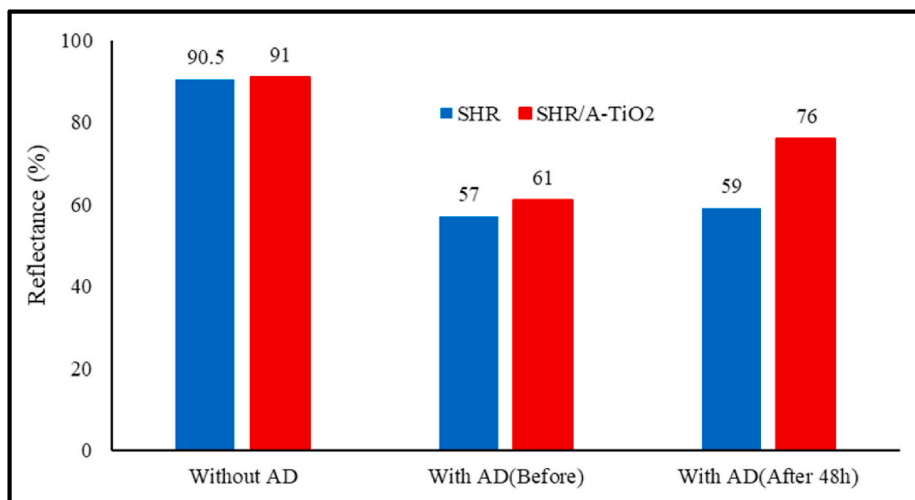


Fig. 10. Average reflectance index values of coating systems with wavelengths in range of 750–1400 nm - before and after 48 h U.V. light irradiation (standard deviation: $\pm 0.2\%$).

Vuong Nguyen: Conceptualization, Methodology, Writing – review & editing, Approval of the version of the manuscript to be published. **Tuan Anh Nguyen:** Writing – original draft, Writing – review & editing, Approval of the version of the manuscript to be published. **Thi Yen Oanh Doan:** Conceptualization, Methodology, Approval of the version of the manuscript to be published. **Thu Ha Hoang:** Formal analysis, Data curation, Approval of the version of the manuscript to be published. **The Tam Le:** Data curation, Approval of the version of the manuscript to be published. **Phuong Nguyen-Tri:** Writing – review & editing, Approval of the version of the manuscript to be published.

Declaration of competing interest

The authors declare that they have no known competing financial interests or personal relationships that could have appeared to influence the work reported in this paper.

Acknowledgments

This work was financially supported by the Vietnam Academy of Science and Technology's Foundation for Material Science (TDVLT.03/21–23).

References

- [1] T.V. Nguyen, P.H. Dao, K.L. Duong, Q.H. Duong, Q.T. Vu, A.H. Nguyen, V.P. Mac, T.L. Le, Effect of R-TiO₂ and ZnO nanoparticles on the UV-shielding efficiency of water-borne acrylic coating, *Prog. Org. Coating* 110 (2017) 114–121.
- [2] Zixiao Wang, Florent Gauvin, Feng Pan, H.J.H. Brouwers, Qingliang Yu - self-cleaning and air purification performance of Portland cement paste with low dosages of nanodispersed TiO₂ coatings, *Construct. Build. Mater.* 263 (2020) 150228.
- [3] T.V. Nguyen, T.V. Do, M.H. Ha, H.K. Le, T.T. Le, T.N.L. Nguyen, X.T. Dam, L.T. Lu, D.L. Tran, Q.T. Vu, D.A. Dinh, T.C. Dang, P. Nguyen -Tri, Crosslinking process, mechanical and antibacterial properties of UV-curable acrylate/Fe₃O₄-Ag nanocomposite coating, *Prog. Org. Coating* 139 (2020) 105325.
- [4] Guifen Fu, S. Patricia, Vary, and Chhiu-Tsu lin - anatase TiO₂ nanocomposites for antimicrobial coatings, *J. Phys. Chem. B* 109 (18) (2005) 8889–8898.
- [5] T.V. Nguyen, P.H. Dao, T.A. Nguyen, V.H. Dang, M.N. Ha, T.T.T. Nguyen, Q.T. Vu, N.L. Nguyen, T.C. Dang, P. Nguyen -Tri, D.L. Tran, L.T. Lu, Photocatalytic degradation and heat reflectance recovery of water-borne acrylic polymer/ZnO nanocomposite coating, *J. Appl. Polym.* (2020), e49116, <https://doi.org/10.1002/app.49116>.
- [6] T.T. Le, T.V. Nguyen, T.A. Nguyen, T.T.H. Nguyen, H. Thai, D.L. Tran, D.A. Dinh, T. M. Nguyen, L.T. Lu, Thermal, mechanical and antibacterial properties of water-based acrylic Polymer/SiO₂-Ag nanocomposite coating, *Mater. Chem. Phys.* 232 (2019) 362–366.
- [7] T.V. Nguyen, T.A. Nguyen, P.H. Dao, V.P. Mac, A.H. Nguyen, M.T. Do, T. H. Nguyen, Effect of rutile titania nanoparticles on the mechanical property, thermal stability, weathering resistance and antibacterial property of styrene acrylic polyurethane coating, *Adv. Nat. Sci-Nanosci.* 7 (4) (2016), 045015-045024.
- [8] T.A. Nguyen, T.H. Nguyen, T.V. Nguyen, H. Thai, X. Shi, Effect of nanoparticles on the thermal and mechanical properties of epoxy coatings, *J. Nanosci.* 16 (2016) 9874–9881.
- [9] T.M.A. Bui, T.V. Nguyen, T.H. Hoang, T.T.H. Nguyen, T.H. Lai, T.N. Tran, V. H. Nguyen, V.H. Hoang, T.L. Le, D.L. Tran, T.C. Dang, Q.T. Vu, T.P. Nguyen, Investigation of crosslinking, mechanical properties and weathering stability of acrylic polyurethane nanocomposite coating reinforced by SiO₂ nanoparticles issued from rice husk ash, *J. Mater. Chem. Phys.* 241 (2020), 122445.
- [10] T.V. Nguyen, P. Nguyen Tri, T.D. Nguyen, R.E. Aidani, V.T. Trinh, C. Decker, Accelerated degradation of water borne acrylic nanocomposites used outdoor protective coatings, *Polym. Degrad. Stabil.* 128 (2016) 65–76.
- [11] P.H. Dao, T.V. Nguyen, M.H. Dang, T.L. Nguyen, V.T. Trinh, V.P. Mac, A. H. Nguyen, M.T. Duong, Effect of silica nanoparticles on properties of coatings based on acrylic emulsion resin, *Vietnam J Sci Technol* 56 (3B) (2018) 117–125.
- [12] Ilaria Alfieri, Andrea Lorenzi, Luca Ranzenigo, Laura Lazzarini, Giovanni Predieri, Pier Paolo Lottici - synthesis and characterization of photocatalytic hydrophobic hybrid TiO₂-SiO₂ coatings for building applications, *Build. Environ.* 111 (2017) 72–79.
- [13] S.S. Latthe, R.S. Sutar, V.S. Kodag, A.K. Bhosale, A.M. Kumar, K.K. Sadasivuni, R. Xing, S. Liu, Self - cleaning super-hydrophobic coatings: potential industrial applications, *Prog. Org. Coating* (2019) 128 52–58.
- [14] Q. Wang, G. Chen, J. Tian, Z. Yu, Q. Deng, M. Yu, Facile fabrication of fluorine-free, transparent and self-cleaning super-hydrophobic coatings based on biopolymer castor oil, *Mater. Lett.* 230 (2018) 84–87.
- [15] Q. Shang, J. Chen, C. Liua, Y. Hua, L. Hua, X. Yang, Y. Zhou, Facile fabrication of environmentally friendly bio-based super-hydrophobic surfaces via UV-polymerization for self-cleaning and high efficient oil/water separation, *Prog. Org. Coating* 137 (2019) 105346.
- [16] C.K. Sumesh, B. Patel, K. Parekh, U.V. light induced photo-degradation of organic dye by ZnO nanocatalysts, *AIP Conf. Proc.* 123 (2013), <https://doi.org/10.1063/1.4810131>.
- [17] B. Li, Y. Shi, J. Cui, Z. Liu, X. Zhang, J. Zhan, Au-coated ZnO nanorods on stainless steel fiber for self-cleaning solid phase microextraction-surface enhanced Raman spectroscopy, *Anal. Chim. Acta* 923 (2016) 66–73.
- [18] S. Banerjee, D.D. Dionysiou, S.C. Pillai, Self-cleaning applications of TiO₂ by photo-induced hydrophilicity and photocatalysis, *Appl. Catal., B* 176–177 (2015) 396–428.
- [19] E. González, A. Bonnefond, M. Barrado, A.M. Casado Barrasa, J.M. Asua, J.R. Leiza, Photoactive self-cleaning polymer coatings by TiO₂ nanoparticle Pickering mini emulsion polymerization, *Chem. Eng. J.* 281 (2015) 209–217.
- [20] L. Yang, S. Zhou, L. Wu, Preparation of water-borne self-cleaning nanocomposite coatings based on TiO₂/PMMA latex, *Prog. Org. Coating* 85 (2015) 208–215.
- [21] B.M. Kalea, J. Wienera, J. Miliitkya, S. Rwwiireaa, R. Mishraa, K.I. Jacobb, Y. Wang, Coating of cellulose-TiO₂ nanoparticles on cotton fabric for durable photocatalytic self-cleaning and stiffness, *Carbohydr. Polym.* 150 (2016) 107–113.
- [22] S. Higashimoto, Titanium-Dioxide-based visible-light-sensitive photocatalysis: mechanistic insight and applications, *Catalysts* 9 (2019) 201, <https://doi.org/10.3390/catal9020201>.
- [23] R. Daghrrir, P. Drogui, D. Robert, Modified TiO₂ for environmental photocatalytic applications: a review -, *Ind. Eng. Chem. Res.* 52 (2013) 3581–3599.
- [24] U.G. Akpan, B.H. Hameed, Parameters affecting the photocatalytic degradation of dyes using TiO₂-based photocatalysts: a review, *J. Hazard Mater.* 170 (2009) 520–529.
- [25] M. Martín, S. Leonid, R. Tomás, S. Jan, K. Jaroslav, K. Mariana, J. Michaela, P. Frantisek, P. Gustav, Anatase TiO₂ nanotube arrays and titania films on titanium

- mesh for photocatalytic NO_x removal and water cleaning, *Catal, Today Off.* 287 (2017) 59–64.
- [26] M.G. Salviaggio, R. Passalacqua, S. Abate, S. Perathoner, G. Centi, M. Lanza, A. Stassi, Functional nano-textured titania-coatings with self-cleaning and antireflective properties for photovoltaic surfaces, *Sol. Energy* 125 (2016) 227–242.
- [27] A.V. Zafir, G. Voicu, A.I. Bădănoiu, D. Gogan, O. Oprea, Eugeniu Vasile, Synthesis and characterization of titania-silica fume composites and their influence on the strength of self-cleaning mortar, *Compos. B Eng.* 140 (2018) 157–163.
- [28] X.D. Chen, Z. Wang, Z.F. Liao, Y.L. Mai, M.Q. Zhang, Roles of anatase and rutile TiO₂ nanoparticles in photooxidation of polyurethane, *Polym. Test.* 26 (2) (2007) 202–208.
- [29] N.S. Allen, M. Edge, A. Ortega, C.M. Liauw, J. Stratton, R.B. McIntyre, Behaviour of nanoparticle (ultrafine) titanium dioxide pigments and stabilisers on the photooxidative stability of water based acrylic and isocyanate based acrylic coatings, *Polym. Degrad. Stabil.* 78 (3) (2002) 467–478.
- [30] D. Kumar, X. Wu, Q. Fu, J. Weng, C. Ho, P.D. Kanhere, L. Li, Z. Chen, Development of durable self-cleaning coatings using organic–inorganic hybrid sol–gel method, *Appl. Surf. Sci.* 344 (2015) 205–212.
- [31] B.W. Johnson, R. McIntyre, Analysis of test methods for UV durability predictions of polymer coatings, *Prog. Org. Coating* 27 (1996) 95–106.
- [32] O. Chiantore, L. Trossarelli, M. Lazzari, Photooxidative degradation of acrylic and methacrylic polymers, *Polymer* 41 (2000) 1657–1668.
- [33] N.S. Allen, C.J. Regana, R. McIntyre, B.W. Johnson, W.A.E. Dunk, The photooxidation and stabilisation of water-borne acrylic emulsions-, *Prog. Org. Coating* 32 (1997) 9–16.
- [34] M. Kolokotroni, E. Shittu, T. Santos, L. Ramowski, A. Mollard, K. Rowe, E. Wilson, J.P.B. Filho, D. Novieto, Cool Roofs, High Tech Low Cost solution for energy efficiency and thermal comfort in low rise low income houses in high solar radiation countries, *Energy Build.* 176 (2018) 58–70.
- [35] Z. Khuzwayo, E.M.N. Chirwa, Analysis of catalyst photo-oxidation selectivity in the degradation of polyorganochlorinated pollutants in batch systems using UV and UV/TiO₂, *S. Afr. J. Chem. Eng.* 23 (2017) 17–25.